tvst

Article

Comparing Fluorescence Lifetime Imaging Ophthalmoscopy in Atrophic Areas of Retinal Diseases

Lukas Goerdt[1,2], Lydia Sauer[1], Alexandra S. Vitale[1], Natalie K. Modersitzki[1], Monika Fleckenstein[1], and Paul S. Bernstein[1]

[1] John A. Moran Eye Center, University of Utah, Salt Lake City, UT, USA
[2] Department of Ophthalmology, University of Bonn, Bonn, Germany

Correspondence: Paul S. Bernstein, John A. Moran Eye Center, University of Utah, 65 Mario Capecchi Drive, Salt Lake City, UT 84132, USA. e-mail: paul.bernstein@hsc.utah.edu

Received: May 28, 2020
Accepted: April 15, 2021
Published: June 10, 2021

Keywords: atrophic retinal diseases; FLIO; fluorescence lifetime imaging; geographic atrophy

Citation: Goerdt L, Sauer L, Vitale AS, Modersitzki NK, Fleckenstein M, Bernstein PS. Comparing fluorescence lifetime imaging ophthalmoscopy in atrophic areas of retinal diseases. Transl Vis Sci Technol. 2021;10(7):11, https://doi.org/10.1167/tvst.10.7.11

Purpose: Fluorescence lifetime imaging ophthalmoscopy (FLIO) is a non-invasive imaging modality to investigate the human retina. This study compares FLIO lifetimes in different degenerative retinal diseases.

Methods: Included were eyes with retinal pigment epithelium (RPE) and/or photoreceptor atrophy due to Stargardt disease ($n = 66$), pattern dystrophy ($n = 18$), macular telangiectasia type 2 ($n = 49$), retinitis pigmentosa ($n = 28$), choroideremia ($n = 26$), and geographic atrophy ($n = 32$) in age-related macular degeneration, as well as 37 eyes of 37 age-matched healthy controls. Subjects received Heidelberg Engineering FLIO, autofluorescence intensity, and optical coherence tomography imaging. Amplitude-weighted mean FLIO lifetimes (τ_m) were calculated and analyzed.

Results: Retinal FLIO lifetimes show significant differences depending on the disease. Atrophic areas in geographic atrophy and choroideremia showed longest mean FLIO lifetimes. τ_m values within areas of RPE and outer nuclear layer atrophy were significantly longer than within areas with preserved outer nuclear layer ($P < 0.001$) or non-atrophic areas ($P < 0.001$).

Conclusions: FLIO is able to contribute additional information regarding differences in chronic degenerative retinal diseases. Although it cannot replace conventional autofluorescence imaging, FLIO adds to the knowledge in these diseases and may help with the correct differentiation between them. This may lead to a more in-depth understanding of the pathomechanisms related to atrophy and types of progression.

Translational Relevance: Differences between atrophic retinal diseases highlighted by FLIO may indicate separate pathomechanisms leading to atrophy and disease progression.

Introduction

Atrophy of photoreceptors and/or the retinal pigment epithelium (RPE) is a common end-stage manifestation of many chronic degenerative retinal diseases. These include but are not limited to geographic atrophy (GA), as the end-stage of non-exudative age-related macular degeneration (AMD), Stargardt disease (STGD), pattern dystrophy, macular telangiectasia type 2 (MacTel), choroideremia, and retinitis pigmentosa (RP). Overall, atrophic retinal diseases lead to severe deterioration of visual acuity.[1,2]

AMD, the leading cause of legal blindness in industrialized countries, typically has a late onset.[3–5] The end stage of non-exudative AMD is referred to as GA and manifests with atrophy of photoreceptors, RPE, and choriocapillaris. There is currently no treatment available for GA.[6,7] Recessive STGD is the most common inherited macular dystrophy.[8] It is caused by a mutation in a retina-specific ATP-binding cassette transporter gene (*ABCA4*), which interferes with the visual cycle and leads to an abnormal accumulation of lipofuscin within the RPE.[8] Atrophic areas can display morphological similarities to GA, bearing the risk of misdiagnosis.[9] Similar to STGD, pattern

dystrophy with *RDS*/*PRPH2*-related gene mutations can also easily be mistaken as GA, as this mutation also leads to apoptosis of the photoreceptors and the RPE.[10–12] The inherited, bilateral, degenerative disease MacTel manifests with loss of the foveolar reflex, the presence of intraretinal cavities and blunting vessels at the fovea, loss of foveal macular pigment, and, subsequently, foveal atrophy.[13–15] Although MacTel has been categorized as a rare disease, recent studies suggest that the number of patients affected by MacTel is underestimated due to frequent misdiagnoses.[16,17] Other retinal diseases that eventually progress to atrophy include choroideremia and RP. Choroideremia is caused by a mutation in the *CHM* gene, which encodes for Rab escort protein 1, a mediator for transmembrane trafficking in the retina and RPE.[18,19] Although central vision is usually preserved, patients suffer from nyctalopia with onset in the first decade of life, progressing peripheral atrophy, and subsequent loss of peripheral vision. Despite a primarily preserved fovea, choroideremia commonly leads to blindness in the late stage of the disease.[20] RP is a genetically determined degenerative disease defined by functional impairment of photoreceptors and RPE, with photoreceptor atrophy.[21,22] In general, rods in the periphery are affected first, followed by central cones, then followed by atrophy of the RPE, ultimately leading to peripheral vision loss and tunnel-like visual fields with progressive constriction.[21,23]

The non-invasive imaging modality fluorescence lifetime imaging ophthalmoscopy (FLIO) may be helpful not only to distinguish different atrophic retinal diseases from another but also to understand their pathophysiology in more detail. First introduced by Schweitzer et al.[24–27] in 2002, FLIO allows for non-invasive imaging of the retina. It has further previously been suggested that FLIO holds the potential to detect subtle metabolic changes in the retina.[24] Different previous FLIO studies have investigated the aforementioned retinal diseases GA, STGD, MacTel, choroideremia, and RP.[28–32] The aim of this study is to comprehensively compare the FLIO characteristics of each individual disease.

Methods

This cross-sectional study was approved by the University of Utah's Institutional Review Board and adhered to the tenets of the Declaration of Helsinki. Patients from the retina clinic at the Moran Eye Center were offered FLIO imaging and inclusion in the study if they were affected by the diseases of interest and showed clear signs of atrophy in optical coherence tomography (OCT) imaging as defined below. Furthermore, patients with pathologic conditions that could interfere with FLIO measurement such as cataract or intra-/subretinal fluid were excluded from this study. Written informed consent was obtained from every patient and from age-matched healthy controls prior to all investigations. All subjects were examined between March 2017 and January 2020 at the Moran Eye Center. Intraocular pressure was measured with a Tono-Pen (Reichart Technologies, Depew, NY), and no topical or intravenous fluorescein was applied before imaging. Pupils were maximally dilated prior to imaging, as this is also important for consistent FLIO imaging.[27,33] Patients received FLIO and OCT imaging (Spectralis OCT, Heidelberg Engineering, Heidelberg, Germany) after pupil dilation.

FLIO Setup and Image Acquisition

Based on the Heidelberg Engineering Spectralis, FLIO records autofluorescence lifetimes in vivo in a 30° retinal field, relying on the principle of time-correlated single-photon counting.[34,35] The detailed setup and safety of FLIO have been described previously.[27,34,36] Briefly, retinal autofluorescence is excited with a pulsed diode laser at 473-nm wavelength, and fluorescence photons are detected with two hybrid photomultipliers (HPM-100-40; Becker & Hickl GmbH, Berlin, Germany). There is only 1 short and one long channel, therefore it is either in short (SSC, 498–560 nm) and long (LSC, 560–720 nm) channels; or, in a short spectral channel (SSC, 498–560 nm) and a long spectral channel (LSC, 560–720 nm). A high-contrast confocal infrared reflectance image is included for eye tracking, and fluorescence photons are recorded at their correct spatial location. To ensure reliable image quality, a minimal signal threshold of at least 1000 photons was recorded for each pixel. Typically, 2 minutes of acquisition time were required for each eye. The repeatability of this technique has previously been confirmed.[25,27,33] The interindividual variability of FLIO has been quantified by the coefficient of variation (CV). The first study found a CV of 17% for the SSC and 11% for the LSC.[27] Two further studies confirmed a good CV of 7.9 in the SSC, and 17.7% in the LSC,[25] as well as 9% to 16% for both channels.[33]

The fluorescence data were analyzed using SPCImage 4.4.2 (Becker & Hickl GmbH), and the mean fluorescence decay was approximated. The amplitude-weighted mean fluorescence decay time (τ_m) was used for further analysis; τ_m represents the average of three time constants from the fit, weighted by their amplitude. Further details have been described elsewhere.[35,36] SPCImage and FLIMX were used to obtain mean FLIO lifetimes over regions of interest.

The FLIMX software is documented and freely available for download online under an open-source BSD license (http://www.flimx.de).[37]

Analyzing Regions of Interest and Grading Atrophy

Structural OCT changes were used to grade atrophy according to the Classification of Atrophy Meetings definition.[38] In brief, complete RPE and outer retinal atrophy (cRORA) was defined by a zone of homogeneous choroidal hypertransmission and absence of the RPE band measuring 250 µm or more with overlying outer retinal thinning and loss of photoreceptors. The size of each lesion was measured and confirmed to be appropriate using the measuring tool implemented in the Heyex OCT software. Terminations of the external limiting membrane and ellipsoid zone had to be visible. Furthermore, we defined areas of homogeneous choroidal hypertransmission due to the absence of RPE, external limiting membrane, and ellipsoid zone with the outer nuclear layer still present as areas of preserved outer retina. These areas were demarcated within the en face infrared image that is routinely obtained with Spectralis OCT imaging. These areas were used as masks on the FLIO measurements; FLIO itself was not used to make any grading.

Unaffected areas were selected using both OCT and autofluorescence intensity imaging. One unaffected area was used per patient. These areas were selected based on the absence of any pathologic retinal manifestation, including but not limited to drusen, atrophy, or presence of fluid. Hyperfluorescent areas were defined as an increased fundus autofluorescence signal compared with autofluorescence signal outside these areas.[39] In healthy eyes, FLIO lifetimes were obtained from the outer ring of the standardized Early Treatment Diabetic Retinopathy Study (ETDRS) grid. Figure 1 depicts where these measurements were taken. Atrophic regions, as well as unaffected areas of interest, were selected manually in each FLIO measurement by drawing the previously defined mask onto the connected autofluorescence intensity image. With SPCImage it is possible to select a manual mask on the autofluorescence intensity image, and the same mask is projected onto the lifetime image at the exact same location of the fundus. Masks over specific areas allowed us to obtain the average of FLIO lifetimes for these areas. As macular pigment is known to influence FLIO lifetimes, only regions of interest outside the direct foveolar area were measured and included in the analysis. Figure 2 shows which exact retinal region of interest was selected for FLIO lifetime measurement in a patient affected by pattern dystrophy.[36]

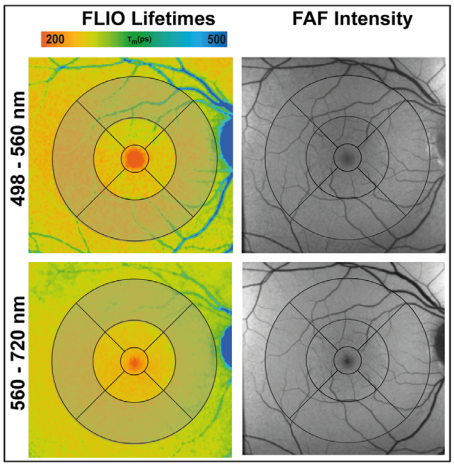

Figure 1. FLIO lifetime image of a healthy 60-year-old female control. The *gray areas* highlight the outer ring of the standardized ETDRS grid from which mean FLIO lifetimes were investigated.

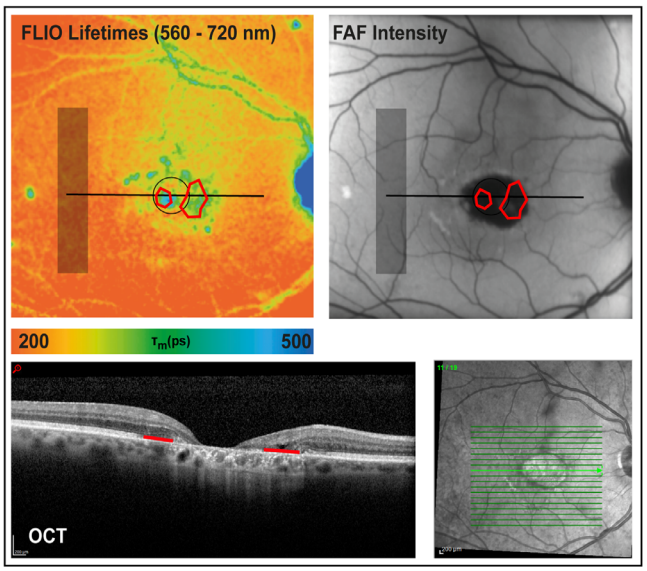

Figure 2. FLIO lifetime image, fundus autofluorescence (FAF) intensity image, and OCT scan of a 61-year-old male patient affected by pattern dystrophy. The *red lines* on the OCT scan highlight where atrophy was graded as cRORA and therefore eligible for FLIO lifetime measurement. The *gray area* depicts where FLIO lifetimes of healthy retinal areas were measured.

Statistical Analysis

For all statistical analyses, SPSS Statistics 21 (IBM, Armonk, NY) and R 3.6.2 were employed. To test for significant τ_m differences between regions in one eye, a *t*-test for paired samples was used. To compare FLIO lifetimes between different patient groups, as well as healthy controls, a *t*-test for independent samples was used. A multiple linear regression analysis accounting for age and lens type was used to compare FLIO lifetimes between patients with different diagnoses.

Assumptions that our diagnosis groups are normally distributed and have equal within-group variance were checked graphically, and a post hoc analysis using Tukey's range test was applied to pairwise compare diagnosis effects on FLIO lifetime while controlling the familywise error rate.[40] All results are reported with their means and standard deviations (SDs).

Results

Subjects

This study investigated 219 eyes from 124 patients. Mean age over all patients was 55 ± 22 years (range, 10–93). Patients with atrophic eye diseases, verified with OCT imaging, were investigated. This included geographic atrophy secondary to AMD (32 eyes), STGD (66 eyes), pattern dystrophy (18 eyes), MacTel (49 eyes), RP (28 eyes), and choroideremia (26 eyes). An age-matched group of 37 eyes from 37 healthy controls with a mean age of 53 ± 19 years (range, 10–85) was included, as well. Table 1 provides further patient information.

Characteristics of Atrophic Eye Diseases in FLIO

In general, atrophic lesions show prolonged FLIO lifetimes. Comparing all atrophies with unaffected retinal areas within the same eye, significant differences were found for both spectral channels. Atrophic areas showed a prolongation of FLIO lifetimes of approximately 150 ps (SSC) and 130 ps (LSC), $P < 0.001$ for both. Comparing FLIO lifetimes of atrophic areas in eyes affected by the aforementioned diseases to FLIO lifetimes in age-matched healthy control eyes, similar differences were found (differences around 140–150 ps in both spectral channels; $P < 0.001$ for both). This is shown in Table 2. Figure 3 presents the different atrophic eye diseases investigated in this study compared with a healthy eye.

Differences Between Different Types of Atrophy

FLIO lifetimes vary among the different types of atrophy. The longest FLIO lifetimes can be found in eyes with GA and choroideremia. All fluorescence-based imaging techniques are impacted by the autofluorescence of the lens. This can be noted especially in patients of an advanced age.[30] Mean lifetimes across atrophic areas from different diseases were compared with each other, controlling for age and lens (natural lens vs. intraocular lens). There was no statistical difference based on the lens status in our study. Significant FLIO lifetime differences in the SSC were found when comparing GA with atrophic areas in MacTel and choroideremia. The SSC also showed significant differences between atrophic areas in choroideremia with atrophic areas in STGD, pattern dystrophies, MacTel, and RP. MacTel and RP also showed significantly different FLIO lifetimes in the SSC. In the LSC, significant differences were found when comparing GA with atrophic areas in STGD, pattern

Table 1. Patient Characteristics

Characteristic	Patients (*n*)	Eyes (*n*)	Age (y), Mean ± SD	Age (y), Range	Gender	Lens
Healthy	37	37	53 ± 19	10–85	16 females (43%); 21 males (57%)	31 natural (84%); 6 intraocular (16%)
All atrophy	124	219	55 ± 21	10–93	53 females (43%); 71 males (57%)	168 natural (77%); 51 intraocular (23%)
GA	21	32	78 ± 11	58–93	8 females (38%); 13 males (62%)	14 natural (44%); 18 intraocular (56%)
STGD	34	66	42 ± 20	11–75	20 females (59%); 14 males (41%)	64 natural (97%); 2 intraocular (3%)
Pattern dystrophy	10	18	54 ± 9	43–69	6 females (60%); 4 males (40%)	18 natural (100%)
MacTel	30	49	61 ± 12	34–83	12 females (40%); 18 males (60%)	40 natural (82%); 9 intraocular (18%)
RP	16	28	60 ± 12	44–77	7 females (44%); 9 males (56%)	6 natural (21%); 22 intraocular (79%)
Choroideremia	13	26	29 ± 14	10–54	13 males (100%)	26 natural (100%)

Table 2. Atrophy Versus Healthy Regions

Test	Channel	Healthy Control (Outer Ring)	Atrophy (Manual Mask)	*P*
Independent sample *t*-test; healthy controls ($n = 37$) vs. patients ($n = 219$)	SSC	248 ± 50 ps	379 ± 183 ps	**0.001**
	LSC	281 ± 50 ps	434 ± 156 ps	**0.001**
Test	Channel	Unaffected Areas (Manual Mask)	Atrophy (Manual Mask)	*P*
Paired sample *t*-test; patients ($n = 219$) vs. patients ($n = 219$)	SSC	226 ± 81 ps	379 ± 183 ps	**0.001**
	LSC	299 ± 89 ps	434 ± 156 ps	**0.001**

Comparison of FLIO lifetimes between healthy controls and eyes affected with atrophy, and between unaffacted and atrophic areas within the same eye. The *P*-values, printed in bold letters, indicate the level of significance.

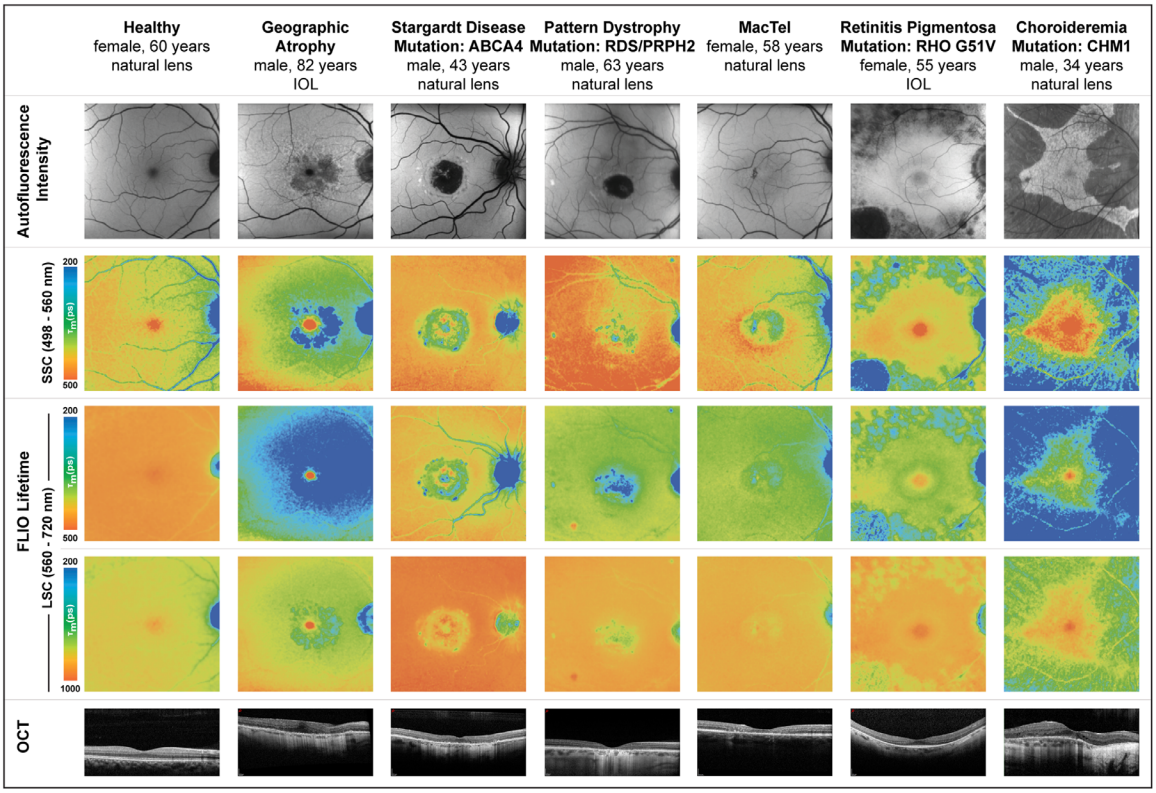

Figure 3. Fundus autofluorescence intensity and FLIO lifetime images from different eyes with atrophic and dystrophic retinal diseases, as well as a healthy control eye. FLIO lifetimes from the SSC and LSC are shown. The LSC is presented in two color ranges.

dystrophies, MacTel, and RP. Furthermore, the LSC also showed significant differences between atrophic areas in choroideremia with atrophic areas in STGD, pattern dystrophies, MacTel, and RP. Statistically significant differences were also found between STGD and MacTel in the LSC. Table 3 shows differences among the different types of atrophy for the SSC and LSC. Figure 4 shows a box plot that highlights these findings.

Difference Between RPE Atrophy and Retinal Atrophy

FLIO lifetimes are typically prolonged in atrophic areas; however, when analyzing RPE atrophy with and without retinal atrophy, differences can be observed. Similarly, retinal atrophy without RPE atrophy, as can be found in RP, also shows different FLIO lifetimes. Areas where the RPE and the outer nuclear layer are

Table 3. Atrophies

A.

Disease	FLIO Lifetimes in Atrophy	
	SSC (498–560 nm)	LSC (560–720 nm)
GA (*n* = 32 eyes)	523 ± 178 ps	609 ± 130 ps
STGD (*n* = 66 eyes)	312 ± 192 ps	385 ± 143 ps
Pattern dystrophy (*n* = 18 eyes)	342 ± 191 ps	397 ± 145 ps
MacTel (*n* = 49 eyes)	319 ± 70 ps	353 ± 59 ps
RP (*n* = 28 eyes)	385 ± 160 ps	413 ± 117 ps
Choroideremia (*n* = 26 eyes)	507 ± 182 ps	540 ± 173 ps

B.

SSC \ LSC	GA	STGD	Pattern Dystrophy	MacTel	RP	Choroideremia
GA		**<0.05**	**<0.01**	**<0.001**	**<0.01**	0.10
STGD	0.31		0.86	**<0.001**	1.0	**<0.001**
Pattern Dystrophy	0.13	0.95		0.39	1.0	**<0.001**
MacTel	**<0.001**	0.20	1.0		0.10	**<0.001**
RP	1.0	0.65	0.39	**<0.05**		**<0.001**
Choroideremia	**<0.05**	**<0.001**	**<0.001**	**<0.001**	**<0.01**	

Part B shows age- and lens-corrected *P* values of differences among the different types of atrophy. White boxes indicate SSC (498–560 nm) and gray boxes indicate LSC (560–720 nm). Bold indicates significance at a $P > 0.05$ level. Tukey's method for comparing a family of six estimates was used for *P* value adjustment.

atrophic show the longest FLIO lifetimes. In areas where the outer nuclear layer is preserved within areas of RPE atrophy, FLIO lifetimes are less prolonged but are still longer than in non-atrophic retinal regions. In areas with preserved RPE but photoreceptor atrophy, FLIO lifetimes appear to be prolonged similarly to complete photoreceptor and RPE atrophy. In conventional autofluorescence imaging, atrophic areas of the RPE appear hypofluorescent compared with areas of healthy retina, regardless of the status of the outer nuclear layer. Moreover, areas of atrophic photoreceptors and preserved RPE display a similarly decreased autofluorescence signal. Figure 5 highlights these findings for the investigated atrophic diseases.

To further quantify these findings, eyes with GA secondary to AMD were segmented according to their atrophy status in correlation with OCT findings. FLIO lifetimes from within segmented areas were compared, Figure 6 gives a detailed example of the aforementioned findings in one patient with GA. Hypofluorescent areas display FLIO lifetimes that depend on the status of the outer nuclear layer. Table 4A shows the statistical analysis, and Figure 7 shows corresponding box plots for both spectral channels.

Finally, we investigated hyperfluorescent areas in different atrophic eye diseases. We found hyperfluorescent areas in eyes with GA, STGD, and pattern dystrophy. Table 4B shows how hyperfluorescent areas differ from other areas within the retina. In GA and STGD, the FLIO lifetimes are significantly shorter in hyperfluorescent areas compared with atrophic areas, whereas FLIO lifetimes are similar between hyperfluorescent areas and atrophic areas in eyes with pattern dystrophy. All hyperfluorescent areas were significantly longer compared with non-atrophic and normal-fluorescent areas.

Characteristics of GA in AMD

Geographic atrophy secondary to non-exudative AMD shows very long FLIO lifetimes in both spectral channels. Comparing all investigated diseases, GA has the longest FLIO lifetimes, ranging from 500 to 700 ps in both spectral channels. In addition, areas surrounding atrophy also show prolonged FLIO lifetimes, and this prolongation occurs in the previously described ring-shaped AMD-related FLIO pattern.[30] Eyes with GA show a more pronounced version of this pattern, which is visible 3 to 6 mm from the fovea. Figure 8 displays a comparison of five eyes affected by GA with five eyes of patients with STGD. All presented patients with STGD had confirmed *ABCA4* mutations.

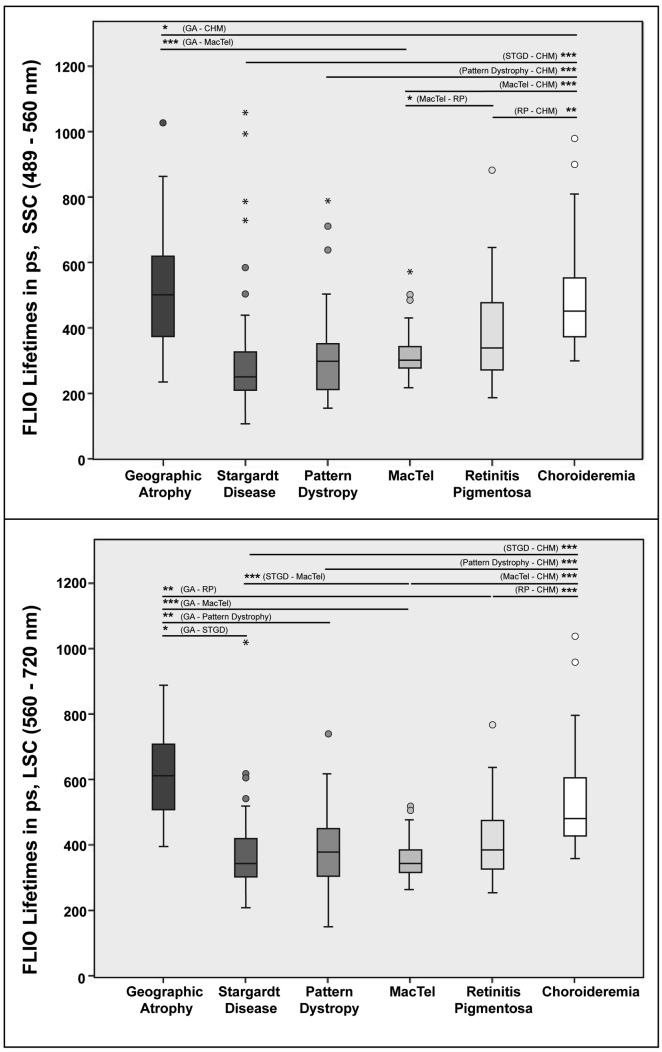

Figure 4. Differences in FLIO lifetimes among different groups of atrophy. Both spectral channels are shown. Lines and asterisks indicate significant differences at $^{*}P < 0.05$ and $^{***}P < 0.001$; $P < 0.05$ was considered significant.

Characteristics of Atrophy in STGD and STGD-Like Pattern Dystrophies

All patients included in the STGD and the pattern dystrophy group had received genetic testing and showed *ELOVL4* or *ABCA4* mutations for STGD or *RDS*/*PRPH2* for pattern dystrophy. Six clinical cases of STGD and four clinical cases of pattern dystrophy were also included in the analysis, because these patients had refused genetic testing or their testing results were still pending. Atrophy in these diseases appeared very similar in small peripheral flecks and in central atrophic regions. In contrast to AMD, shorter lifetimes were observed both within atrophic areas and in surrounding non-atrophic areas. None of these eyes showed the AMD-related FLIO pattern. Figure 8 shows five cases of STGD in patients with confirmed *ABCA4* mutations.

Characteristics of Atrophy in MacTel

Atrophic disease may manifest in advanced MacTel and typically starts temporal to the fovea. In general, FLIO shows a temporal crescent or a ring-like pattern of prolonged lifetimes around the fovea, with the longest lifetimes typically being found temporally. Lifetimes are explicitly more prolonged in the SSC, being a unique feature, as other atrophic retinal diseases tend to display more prolonged FLIO lifetimes in the LSC. Atrophy typically remains within the MacTel area, sparing peripheral retinal regions.

Characteristics of Atrophy in RP

All patients diagnosed with RP had received confirmatory genetic testing, and different genotypes were included in this study. Characteristically, FLIO shows prolonged lifetimes in atrophic areas of the retinal periphery. Atrophy typically includes the photoreceptors but spares the RPE. These atrophic areas typically manifest in a speckled manner, further progressing concentrically toward the fovea. Central retinal areas with preserved RPE and outer nuclear layers show shorter FLIO lifetimes. Figure 9 gives an example of three eyes affected by RP.

Characteristics of Atrophy in Choroideremia

All patients underwent genetic testing to confirm a mutation in the *CHM* gene. Alongside GA, choroideremia showed extremely prolonged FLIO lifetimes in atrophic areas, even in very young patients. These lifetimes increase with age. Prolonged lifetimes can be observed, especially in the periphery, where RPE atrophy and atrophy of the outer nuclear layers occur. Areas with non-atrophic outer nuclear layers according to the applied grading system, often displaying outer retinal tubulations, retain shorter FLIO lifetimes. Further, FLIO images of choroideremia typically do not follow the appearance of the disease in fundus autofluorescence (FAF) intensity imaging. Some areas that appear normal or hyperfluorescent in FAF intensity imaging show prolonged FLIO lifetimes. Figure 9 gives an example of such eyes affected by choroideremia that highlights these findings. Compared with other peripheral atrophies (e.g., RP), which display a rather speckled structure, eyes affected by choroideremia appear streaky in FLIO imaging.

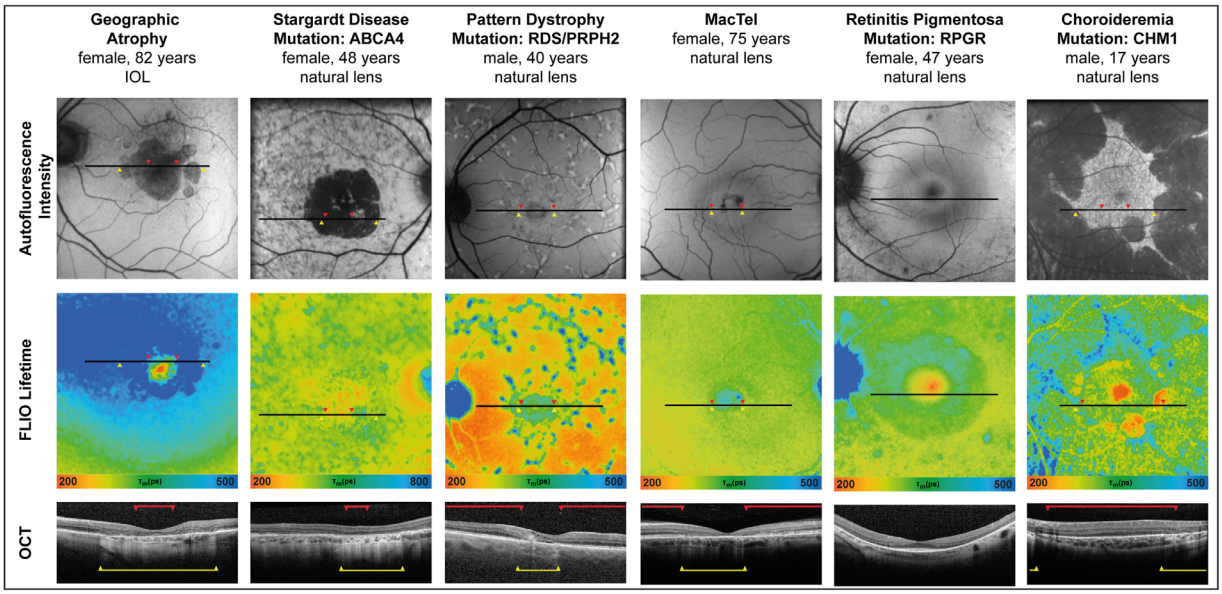

Figure 5. Autofluorescence intensity and FLIO lifetime images from the LSC (560–720 nm) and OCT images in atrophic eye diseases. *Yellow arrows* and *lines* indicate RPE atrophy; *red arrows* and *lines* indicate RPE atrophy with a preserved outer nuclear layer.

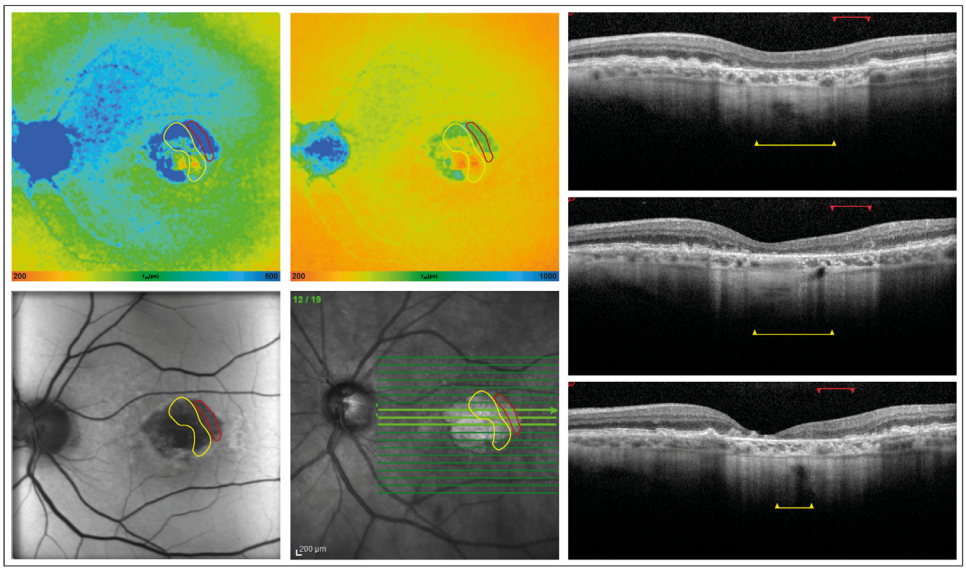

Figure 6. Autofluorescence intensity and FLIO lifetime images in one patient with GA from the LSC (560–720 nm). FLIO images are shown in two different color ranges. *Yellow lines* indicate RPE with outer nuclear layer atrophy, and *red lines* delineate regions with RPE atrophy but without outer nuclear layer atrophy.

Discussion

Conventional imaging, such as autofluorescence intensity imaging, often shows hypofluorescence in atrophic areas, but a differentiation of areas with a preserved outer nuclear layer is difficult.[41] In contrast, OCT has been shown to be helpful in understanding how the morphology of individual layers change.[42] FLIO may contribute additional information to conventional imaging modalities.[24,43]

In general, atrophic areas of any kind present with prolonged FLIO lifetimes.[28,29,43] The exact prolongation may be correlated with types of atrophy and individual disease pathomechanisms. In GA, FLIO lifetimes are significantly longer in atrophic areas of the

Table 4. Hyperfluorescent Areas, RPE Atrophy With and Without Outer Nuclear Layer Atrophy in GA, STGD, and Pattern Dystrophy

A.

Channel	RPE Atrophy With Outer Nuclear Layer Atrophy	RPE Atrophy Without Outer Nuclear Layer Atrophy	Unaffected Areas	*P*
SSC	589 ± 178 ps	431 ± 173 ps	327 ± 79 ps	**<0.001**
LSC	687 ± 159 ps	550 ± 160 ps	417 ± 75 ps	**<0.001**

B.

Disease	Channel	Hyperfluorescent Areas	Atrophic Areas	*P*
GA ($n = 32$ eyes)	SSC	388 ± 99 ps	523 ± 178 ps	**<0.001**
	LSC	507 ± 88 ps	609 ± 130 ps	**<0.001**
STGD ($n = 66$ eyes)	SSC	285 ± 81 ps	301 ± 169 ps	0.327
	LSC	352 ± 81 ps	385 ± 143 ps	**<0.05**
Pattern dystrophy ($n = 18$ eyes)	SSC	295 ± 61 ps	342 ± 191 ps	0.271
	LSC	338 ± 74 ps	397 ± 145 ps	0.117

Disease	Channel	Hyperfluorescent Areas	Non-Atrophic, Normal Fluorescent Areas	*P*
GA ($n = 32$ eyes)	SSC	388 ± 99 ps	322 ± 79 ps	**<0.001**
	LSC	507 ± 88 ps	421 ± 75 ps	**<0.001**
STGD ($n = 66$ eyes)	SSC	285 ± 81 ps	197 ± 70 ps	**<0.001**
	LSC	352 ± 81 ps	268 ± 89 ps	**<0.001**
Pattern dystrophy ($n = 18$ eyes)	SSC	295 ± 61 ps	233 ± 44 ps	**<0.001**
	LSC	338 ± 74 ps	283 ± 49 ps	**<0.01**

Part A shows results from an analysis of variance among the different atrophic areas, specifically areas with RPE atrophy with and without outer nuclear layer atrophy, compared with unaffected areas. Part B shows Bonferroni-corrected *P* values of differences between hyperfluorescent areas and atrophic areas, as well as hyperfluorescent areas and unaffected areas. Both spectral channels (SSC, 498–560 nm; LSC, 560–720 nm) are shown.

retina compared to non-affected areas.[28,31] Similarly, atrophic areas in STGD display longer lifetimes than healthy retinal areas.[29] However, FLIO lifetimes within atrophic areas are significantly longer in GA compared to STGD.[32] In MacTel, FLIO shows a crescent-shaped area of prolonged lifetimes temporal to the fovea. Advanced disease stages, however, show the shape of a ring surrounding the fovea.[44] In advanced atrophic stages of the disease, the prolonged FLIO lifetimes can affect the complete MacTel area.[44] In other atrophic diseases, such as RP and choroideremia, it has been found that FLIO lifetimes are not uniformly prolonged.[45–47] It has been suggested that an intact outer nuclear layer in choroideremia, which may be preserved despite RPE atrophy, may be the reason for relatively normal FLIO lifetimes. In RP, however, areas of photoreceptor atrophy and preserved RPE display significantly prolonged FLIO lifetimes, similar to atrophies with complete RPE and photoreceptor atrophy.

When comparing all types of atrophy, FLIO lifetimes in GA and choroideremia are much longer compared with other diseases that we investigated. In these two conditions, choroidal atrophy results in a complete loss of retinal layers and function.[48,49] In other diseases, lifetimes remain within shorter ranges, indicating that some retinal areas may still be preserved. Furthermore, some areas within atrophy may even show short to normal FLIO lifetimes. We found that significantly shorter lifetimes were originating from areas with a preserved outer nuclear layer, compared with areas of complete RPE and outer nuclear layer atrophy, as in GA and choroideremia. Two previous FLIO studies investigated patients with choroideremia.[47,50] In one study, the authors argued that the short FLIO lifetimes may originate from an accumulation of the visual cycle byproduct all-*trans* retinal, which typically shows short fluorescence lifetimes.[51] According to the authors, this could indicate preserved metabolic activity in the

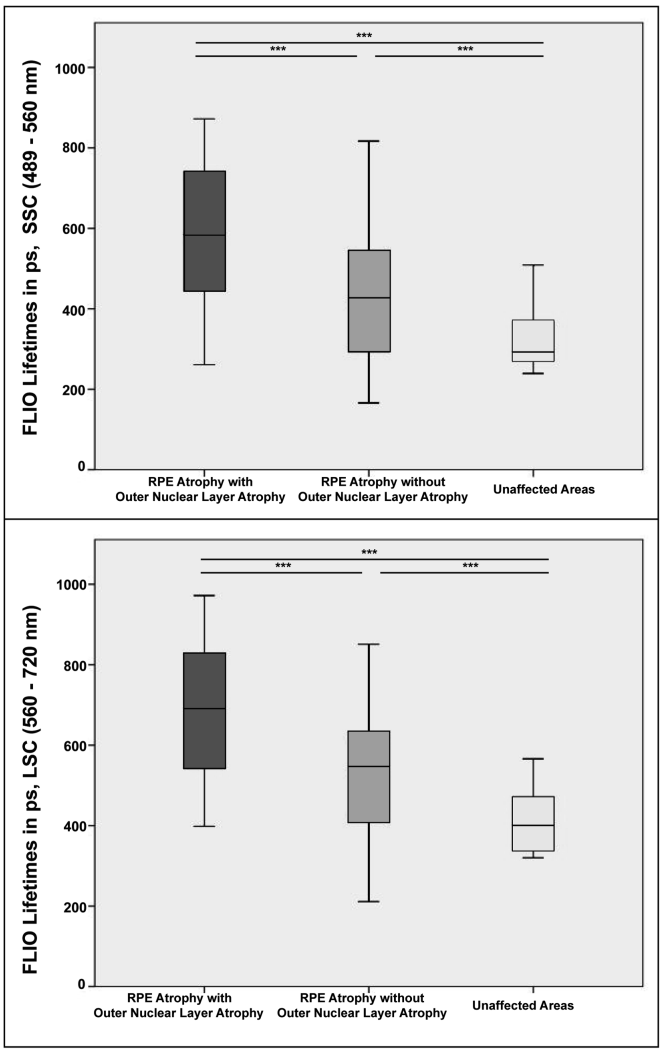

Figure 7. Box plots indicating differences in FLIO lifetimes among areas of RPE atrophy with outer nuclear layer atrophy, RPE atrophy without outer nuclear layer atrophy, and unaffected areas. Lines indicate significant differences at $^{***}P < 0.001$. $P < 0.05$ was considered significant.

photoreceptors. Pfau and colleagues[52] found preserved light sensitivity in border regions within the atrophic areas of GA, whereas Foote and colleagues[53] demonstrated similar results in patients affected by choroideremia. The border regions within atrophic areas of GA and choroideremia also show short FLIO lifetimes, as has been shown in previous FLIO studies.[30,31] A second FLIO study on patients with choroideremia found short FLIO lifetimes originating from areas with outer retinal tubulations.[50] Short FLIO lifetimes within atrophic retinal areas may indicate areas of at least partially preserved photoreceptor structure, which eventually might indicate preserved photoreceptor function. This might be an interesting finding to consider when identifying patients who might benefit from enrollment in early clinical trials.[54,55]

Hyperfluorescent areas have previously been described as areas at risk for atrophy progression.[39] In GA, FLIO lifetimes of the hyperfluorescent junctional zone were significantly shorter compared with atrophic areas and were significantly longer compared with non-atrophic retinal areas without hyperfluorescence.[28] This could indicate pathological changes already happening in hyperfluorescent areas, predisposing the concerned cells for subsequent atrophy; however, it may still be possible to preserve these areas from complete atrophy. Histologically, pathological changes in the RPE also increase with increasing proximity to atrophic regions.[56] In choroideremia, normal or hyperfluorescent areas of RPE already show prolonged FLIO lifetimes, which may indicate cellular processes in these areas that may be related to disease progression. Especially in choroideremia, FLIO shows alterations in areas that in FAF intensity imaging may appear normal. This important finding was further evaluated in a different study.[50]

Furthermore, various retinal diseases are often misclassified.[9,16,17] In some cases, it can be challenging to correctly distinguish a patient with GA secondary to AMD from a patient with late-onset STGD.[9] Similarly, many patients with atrophic MacTel have been misdiagnosed as having atrophic AMD or other retinal diseases.[16,17] By showing a very characteristic pattern of FLIO lifetimes in the LSC, FLIO can help to distinguish among these diseases.[44] The AMD pattern is found in the LSC and shows a ring of prolonged FLIO lifetimes between 3 mm and 6 mm from the fovea.[30] This pattern was found in patients with both exudative and non-exudative AMD, and we can confirm it for patients with GA, as well. In MacTel, a different pattern can be found.[44,57] The FLIO pattern in MacTel appears in the SSC as a temporal area of prolonged FLIO lifetimes, which is typically not exceeding the MacTel area of approximately 5° vertical and 6° horizontal eccentricities.[13] Regarding choroideremia, we were able to confirm findings from a previous study indicating that its appearance in FLIO and autofluorescence intensity imaging are not necessarily concordant.[47] Dysli and colleagues[47] argued that this could be explained by an increased accumulation of lipofuscin derivatives, sustaining the assumption that the RPE is first to degenerate in the course of choroideremia. Finally, FLIO lifetimes show different patterns when comparing RP with choroideremia. Not only are FLIO lifetimes in choroideremia much longer than in RP, but they also show phenotypical differences. FLIO lifetimes in RP appear speckled, whereas FLIO lifetimes in choroideremia appear streaky. To this point, we can only speculate on the reasons for this. The streaky appearance resembles the structure of

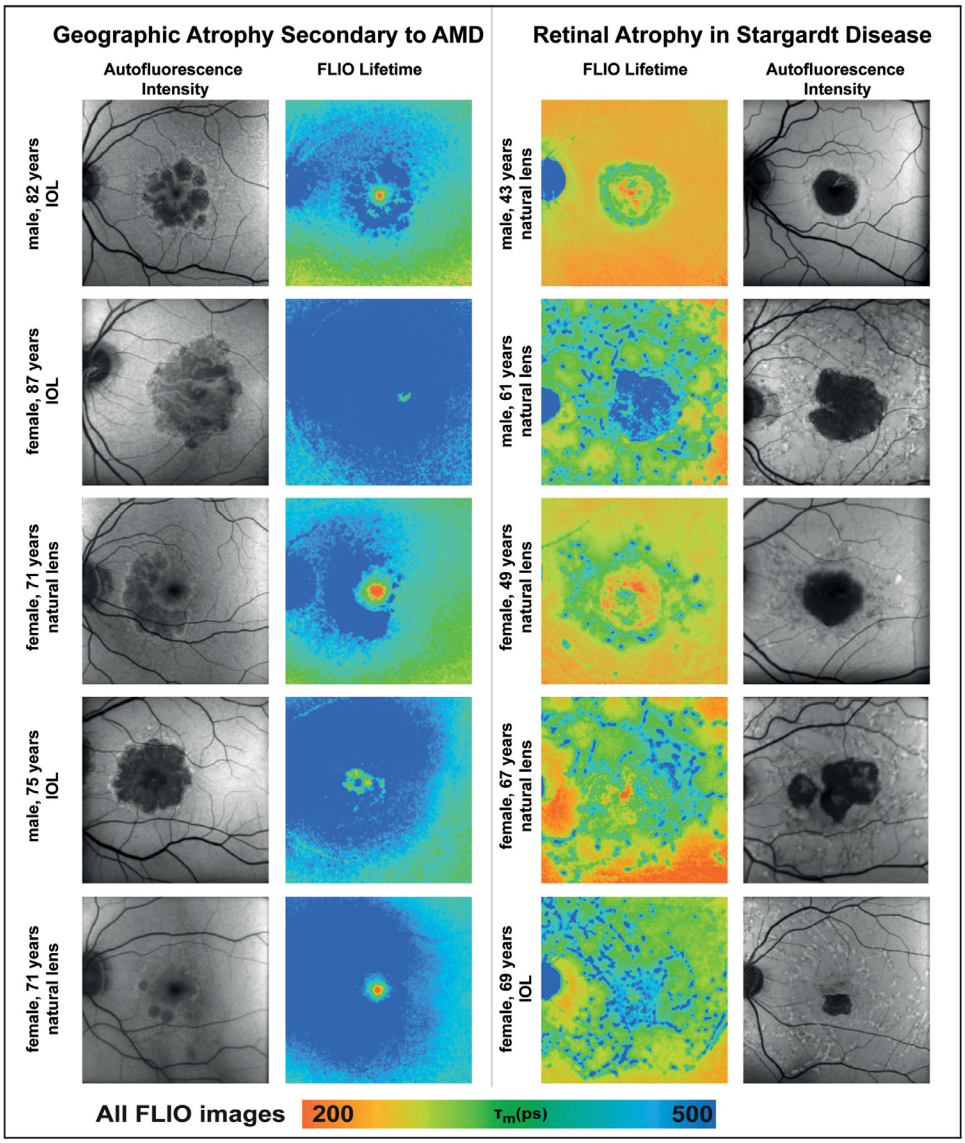

Figure 8. Autofluorescence intensity and FLIO lifetime images in patients with GA and atrophy due to STGD from the LSC (560–720 nm). Phenotypically, FLIO shows the AMD ring in patients with AMD but not in patients with STGD.

choroidal vessels, suggesting a choroidal contribution to the FLIO lifetimes examined in this study. The differences in appearance between RP and choroideremia could help to further understand the pathomechanisms involved in these diseases and provide information on how diseases progress. It may also highlight the different types of atrophy in these diseases, as choroideremia presents with RPE and photoreceptor atrophy, whereas the RPE is mostly preserved in RP.

This study has a several limitations. These include small patient numbers in some investigated subgroups, such as pattern dystrophy. Another limitation lies in the fact that all fluorescence-based imaging modalities are influenced by the lens to a certain degree. In this study, we excluded patients with cataracts. Previous studies have shown that lens status mainly impacts the SSC, leaving the LSC unaffected.[28] A statistical analysis controlling for the lens status did not show significant differences in patients with IOL compared with those with a natural lens. Future studies should further assess the impact of lenses on FLIO lifetimes in a more in-depth manner. Furthermore, axial length has not been assessed in our study, and assessing the axial length was not part of the current study protocol. Despite not yet being investigated, an influence on FLIO measurements is possible and should be addressed in future studies. Best-corrected visual acuity, central macular thickness, and foveal sparing were not assessed in this study, as these parameters depend on the state of the fovea, which was deliberately excluded from the

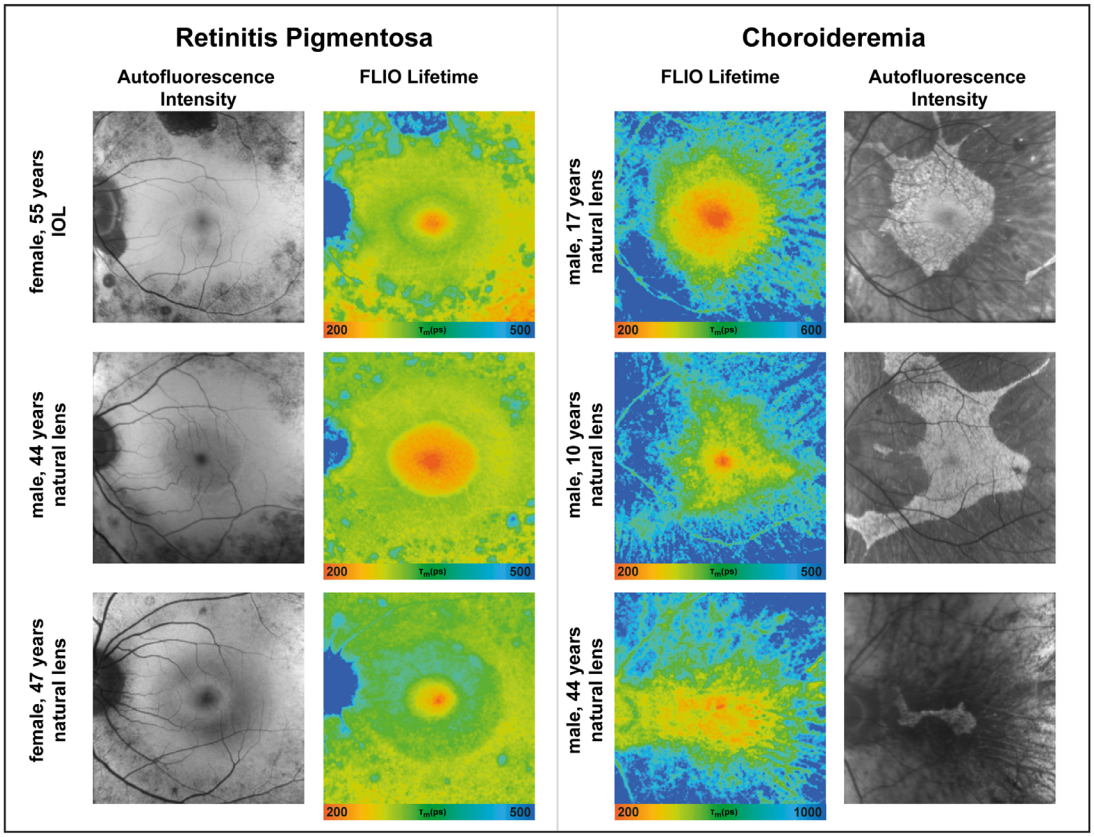

Figure 9. Autofluorescence intensity and FLIO lifetime images in patients with RP and choroideremia from the LSC (560–720 nm). Phenotypical differences in atrophic appearance between RP and choroideremia are visible in FLIO images. Although eyes with RP show atrophy in a speckled form, atrophy in choroideremia appears in a streaky pattern.

analysis.[58] Studies investigating foveal FLIO lifetimes in atrophic retinal diseases should investigate these parameters, which could be very interesting, as they would likely differ between eyes with and without foveal sparing. The reproducibility of FLIO has been investigated in various studies by multiple groups, all of which found a similar reproducibility with a coefficient of variation between 9% and 17%. We verified this reproducibility for our FLIO device; however, these data are currently unpublished.[25,27,33]

We included and compared patients of different age ranges. This is due to the fact that different diseases may manifest at different ages. FLIO lifetimes, especially those of the SSC, were found to be influenced by age.[59] We therefore had an age-matched group of healthy subjects for each disease. Furthermore, we controlled for age in our statistical analysis, which should minimize this impact on our statistical results. One can further speculate about an impact of time since diagnosis on FLIO lifetimes. In this study, we did not assess for the initial date of diagnosis nor did we collect information on time since the development of atrophy. Future studies should be conducted to investigate this. Nevertheless, all included eyes showed atrophic diseases, which we believe is a similarity that makes comparing these diseases important.

Conclusions

Atrophic retinal diseases appear differently in FLIO, and this imaging modality gives additional information relative to conventional fundus autofluorescence intensity imaging. Atrophy typically shows prolonged FLIO lifetimes, but different types of atrophy show different types of FLIO lifetime prolongation. Areas of preserved outer nuclear layers, for example, remain with less prolonged FLIO lifetimes. In FAF intensity imaging, most areas of atrophy appear similar. The information obtained with FLIO may therefore be useful in clinical trials and may give further information on the pathogenesis of the different diseases. Finally, FLIO aids in distinguishing among the different atrophic diseases and may help to avoid misclassification of atrophic eye conditions.

Acknowledgments

The authors thank Heidelberg Engineering for providing the FLIO and for their technical assistance; they especially thank Yoshihiko Katayama, PhD. The authors thank all co-workers from the John A. Moran Eye Center who helped recruit and image patients, as well as Benjamin Brintz, PhD, for statistical assistance.

Supported by grants from the National Institutes of Health (EY11600 and EY14800) and by Lowy Medical Research Institute and Research to Prevent Blindness. This investigation was also supported by the University of Utah Population Health Research Foundation, with funding obtained in part from the National Center for Research Resources and the National Center for Advancing Translational Sciences, National Institutes of Health, through Grant UL1TR002538 (formerly 5UL1TR001067-05, 8UL1TR000105, and UL1RR025764). The funding organizations had no role in the design or conduct of this research. Heidelberg Engineering provided the FLIO instrument to the University of Utah at no cost.

Disclosure: **L. Goerdt**, Heidelberg Engineering (F), Optos (F), Carl Zeiss Meditec (F), CenterVue (F), Novartis (F); **L. Sauer**, Novartis (C), Tesseract Health (C); **A.S. Vitale**, Tesseract Health (C); **N.K. Modersitzki**, None; **M. Fleckenstein**, Novartis (F, C), Heidelberg Engineering (F), STZ GRADE Reading Center (E), Genentech/Roche (C), Ophthalmo Update GmbH (C), pending patent (US20140303013A1); **P.S. Bernstein**, Tesseract Health (C)

References

1. Sunness JS. The natural history of geographic atrophy, the advanced atrophic form of age-related macular degeneration. *Mol Vis*. 1999;5(25):20–25.
2. Stargardt K. Über familiäre, progressive Degeneration in der Maculagegend des Auges. *Albr von Graefes Arch für Ophthalmol*. 1909;71(3):534–550.
3. Attebo K, Mitchell P, Smith W. Visual acuity and the causes of visual loss in Australia. The Blue Mountains Eye Study. *Ophthalmology*. 1996;103(3):357–364.
4. Holz FG, Bindewald-Wittich A, Fleckenstein M, Dreyhaupt J, Scholl HPN, Schmitz-Valckenberg S. Progression of geographic atrophy and impact of fundus autofluorescence patterns in age-related macular degeneration. *Am J Ophthalmol*. 2007;143(3):463–472.
5. Klein R, Klein BEK, Cruickshanks KJ. The prevalence of age-related maculopathy by geographic region and ethnicity. *Prog Retin Eye Res*. 1999;18(3):371–389.
6. Rudnicka AR, Kapetanakis VV, Jarrar Z, et al. Incidence of late-stage age-related macular degeneration in American whites: systematic review and meta-analysis. *Am J Ophthalmol*. 2015;160(1):85–93.e3.
7. Chaikitmongkol V, Tadarati M, Bressler NM. Recent approaches to evaluating and monitoring geographic atrophy. *Curr Opin Ophthalmol*. 2016;27(3):217–223.
8. Cideciyan AV, Aleman TS, Swider M, et al. Mutations in ABCA4 result in accumulation of lipofuscin before slowing of the retinoid cycle: a reappraisal of the human disease sequence. *Hum Mol Genet*. 2004;13(5):525–534.
9. Lambertus S, Lindner M, Bax NM, et al. Progression of late-onset Stargardt disease. *Invest Ophthalmol Vis Sci*. 2016;57(13):5186–5191.
10. Ozkaya A, Garip R, Nur Tarakcioglu H, Alkin Z, Taskapili M. Clinical and imaging findings of pattern dystrophy subtypes; diagnostic errors and unnecessary treatment in clinical practice. *J Fr Ophtalmol*. 2018;41(1):21–29.
11. Toto L, Borrelli E, Mastropasqua R, et al. Adult-onset foveomacular vitelliform dystrophy evaluated by means of optical coherence: a comparison with dry age-related macular degeneration and healthy eyes. *Retina*. 2018;38(4):731–738.
12. Farjo R, Naash MI. The role of Rds in outer segment morphogenesis and human retinal disease. *Ophthalmic Genet*. 2006;27(4):117–122.
13. Charbel Issa P, Gillies MC, Chew EY, et al. Macular telangiectasia type 2. *Prog Retin Eye Res*. 2013;34:49–77.
14. Gass JD, Oyakawa RT. Idiopathic juxtafoveolar retinal telangiectasis. *Arch Ophthalmol*. 1982;100(5):769–780.
15. Helb HM, Charbel Issa P, Van Der Veen RLP, Berendschot TTJM, Scholl HPN, Holz FG. Abnormal macular pigment distribution in type 2 idiopathic macular telangiectasia. *Retina*. 2008;28(6):808–816.
16. Sallo FB, Leung I, Mathenge W, et al. The prevalence of type 2 idiopathic macular telangiectasia in two African populations. *Ophthalmic Epidemiol*. 2012;19(4):185–189.
17. Klein R, Blodi BA, Meuer SM, Myers CE, Chew EY, Klein BEK. The prevalence of macular telangiectasia type 2 in the Beaver Dam Eye Study. *Am J Ophthalmol*. 2010;150(1):55–62.

18. Seabra MC, Brown MS, Slaughter CA, Südhof TC, Goldstein JL. Purification of component A of Rab geranylgeranyl transferase: Possible identity with the choroideremia gene product. *Cell*. 1992;70(6):1049–1057.
19. Sanchez-Alcudia R, Garcia-Hoyos M, Lopez-Martinez MA, et al. A comprehensive analysis of choroideremia: from genetic characterization to clinical practice. *PLoS One*. 2016;11(4): e0151943.
20. Zinkernagel MS, MacLaren RE. Recent advances and future prospects in choroideremia. *Clin Ophthalmol*. 2015;9:2195–2200.
21. Murakami T, Akimoto M, Ooto S, et al. Association between abnormal autofluorescence and photoreceptor disorganization in retinitis pigmentosa. *Am J Ophthalmol*. 2008;145(4):687–694.
22. Fishman GA. Retinitis pigmentosa: visual loss. *Arch Ophthalmol*. 1978;96(7):1185–1188.
23. Hamel C. Retinitis pigmentosa. *Orphanet J Rare Dis*. 2006;1(1):40.
24. Dysli C, Wolf S, Berezin MY, Sauer L, Hammer M, Zinkernagel MS. Fluorescence lifetime imaging ophthalmoscopy. *Prog Retin Eye Res*. 2017;60:120–143.
25. Klemm M, Dietzel A, Haueisen J, Nagel E, Hammer M, Schweitzer D. Repeatability of autofluorescence lifetime imaging at the human fundus in healthy volunteers. *Curr Eye Res*. 2013;38(7):793–801.
26. Schweitzer D, Hammer M, Schweitzer F, et al. In vivo measurement of time-resolved autofluorescence at the human fundus. *J Biomed Opt*. 2004;9(6):1214–1222.
27. Dysli C, Quellec G, Abegg M, et al. Quantitative analysis of fluorescence lifetime measurements of the macula using the fluorescence lifetime imaging ophthalmoscope in healthy subjects. *Invest Ophthalmol Vis Sci*. 2014;55(4):2106–2113.
28. Dysli C, Wolf S, Zinkernagel MS. Autofluorescence lifetimes in geographic atrophy in patients with age-related macular degeneration. *Invest Ophthalmol Vis Sci*. 2016;57(6):2479–2487.
29. Dysli C, Wolf S, Hatz K, Zinkernagel MS. Fluorescence lifetime imaging in Stargardt disease: potential marker for disease progression. *Invest Ophthalmol Vis Sci*. 2016;57(3):832–841.
30. Sauer L, Gensure RH, Andersen KM, et al. Patterns of fundus autofluorescence lifetimes in eyes of individuals with nonexudative age-related macular degeneration. *Invest Ophthalmol Vis Sci*. 2018;59(4):AMD65–AMD77.
31. Sauer L, Klemm M, Peters S, et al. Monitoring foveal sparing in geographic atrophy with fluorescence lifetime imaging ophthalmoscopy - a novel approach. *Acta Ophthalmol*. 2018;96(3):257–266.
32. Solberg Y, Dysli C, Escher P, Berger L, Wolf S, Zinkernagel MS. Fluorescence lifetime patterns of retinal pigment epithelium atrophy in patients with Stargardt disease and age-related macular degeneration. *Ophthalmologica*. 2019;243(3):195–206.
33. Kwon S, Borrelli E, Fan W, Ebraheem A, Marion KM, Sadda SR. Repeatability of fluorescence lifetime imaging ophthalmoscopy in normal subjects with mydriasis. *Transl Vis Sci Technol*. 2019;8(3):15.
34. Schweitzer D, Kolb A, Hammer M, Anders R. Time-correlated measurement of autofluorescence. A method to detect metabolic changes in the fundus. *Ophthalmologe*. 2002;99(10):774–779.
35. Becker W. *The bh TCSPC Handbook*. 4th ed. Berlin: Becker & Hickl GmbH; 2010.
36. Sauer L, Schweitzer D, Ramm L, Augsten R, Hammer M, Peters S. Impact of macular pigment on fundus autofluorescence lifetimes. *Invest Ophthalmol Vis Sci*. 56(8):4668–4679.
37. Klemm M, Schweitzer D, Peters S, Sauer L, Hammer M, Haueisen J. Impact of macular pigment on fundus autofluorescence lifetimes. FLIMX: a software package to determine and analyze the fluorescence lifetime in time-resolved fluorescence data from the human eye. *PLoS One*. 10(7):e0131640.
38. Sadda SR, Guymer R, Holz FG, et al. Consensus definition for atrophy associated with age-related macular degeneration on OCT: Classification of Atrophy Report 3. *Ophthalmology*. 2018;125(4):537–548.
39. Holz FG, Bellman C, Staudt S, Schu¨tt F, Vo¨lcker HE. Fundus autofluorescence and development of geographic atrophy in age-related macular degeneration. *Invest Ophthalmol Vis Sci*. 2001;42(5):1051–1056.
40. Tukey JW. Comparing individual means in the analysis of variance. *Biometrics*. 1949;5(2):99–114.
41. Lindner M, Böker A, Mauschitz MM, et al. Directional kinetics of geographic atrophy progression in age-related macular degeneration with foveal sparing. *Ophthalmology*. 2015;122:1356–1365.
42. Rangaswamy NV, Patel HM, Locke KG, Hood DC, Birch DG. A comparison of visual field sensitivity to photoreceptor thickness in retinitis pigmentosa. *Invest Ophthalmol Vis Sci*. 2010;51(8):4213–4219.
43. Sauer L. Review of clinical approaches in fluorescence lifetime imaging ophthalmoscopy. *J Biomed Opt*. 2018;23(9):1–20.
44. Sauer L, Gensure RH, Hammer M, Bernstein PS. Fluorescence lifetime imaging ophthalmoscopy: a

novel way to assess macular telangiectasia type 2. *Ophthalmol Retin*. 2018;2(6):587–598.
45. Andersen KM, Sauer L, Gensure RH, Hammer M, Bernstein PS. Characterization of retinitis pigmentosa using fluorescence lifetime imaging ophthalmoscopy (FLIO). *Transl Vis Sci Technol*. 2018;7(3):20.
46. Dysli C, Schürch K, Pascal E, Wolf S, Zinkernagel MS. Fundus autofluorescence lifetime patterns in retinitis pigmentosa. *Invest Ophthalmol Vis Sci*. 2018;59(5):1769–1778.
47. Dysli C, Wolf S, Tran HV, et al. Autofluorescence lifetimes in patients with choroideremia identify photoreceptors in areas with retinal pigment epithelium atrophy. *Invest Ophthalmol Vis Sci*. 2016;57(15):6714–6721.
48. MacDonald IM, Russell L, Chan CC. Choroideremia: new findings from ocular pathology and review of recent literature. *Surv Ophthalmol*. 2009;54(3):401–407.
49. Fleckenstein M, Mitchell P, Freund KB, et al. The progression of geographic atrophy secondary to age-related macular degeneration. *Ophthalmology*. 2017;125(3):369–390.
50. Vitale AS, Sauer L, Modersitzki NK, Bernstein PS. Fluorescence lifetime imaging ophthalmoscopy (FLIO) in patients with choroideremia. *Transl Vis Sci Technol*. 2020;9(10):33.
51. Loguinova MY, Zagidullin VE, Feldman TB, et al. Spectral characteristics of fluorophores formed via interaction between all-trans-retinal with rhodopsin and lipids in photoreceptor membrane of retina rod outer segments. *Biochem Suppl Ser A Membr Cell Biol*. 2009;3(2):134–143.
52. Pfau M, Von Der Emde L, Dysli C, et al. Light sensitivity within areas of geographic atrophy secondary to age-related macular degeneration. *Invest Ophthalmol Vis Sci*. 2019;60(12):3992–4001.
53. Foote KG, Rinella N, Tang J, et al. Cone structure persists beyond margins of short-wavelength autofluorescence in choroideremia. *Invest Ophthalmol Vis Sci*. 2019;60(14):4931–4942.
54. Schwartz SD, Tan G, Hosseini H, Nagiel A. Subretinal transplantation of embryonic stem cell–derived retinal pigment epithelium for the treatment of macular degeneration: an assessment at 4 years. *Invest Ophthalmol Vis Sci*. 2016;57(5):ORSFc1–ORSFc9.
55. Kashani AH, Lebkowski JS, Rahhal FM, et al. A bioengineered retinal pigment epithelial monolayer for advanced, dry age-related macular degeneration. *Sci Transl Med*. 2018;10(435):eaao4097.
56. Zanzottera EC, Ach T, Huisingh C, Messinger JD, Freund KB, Curcio CA. Visualizing retinal pigment epithelium phenotypes in the transition to atrophy in neovascular age-related. *Retina*. 2016;36(12):26–39.
57. Solberg Y, Dysli C, Wolf S, Zinkernagel MS. Fluorescence lifetime patterns in macular telangiectasia type 2. *Retina*. 2020;40(1):99–108.
58. Lindner M, Nadal J, Mauschitz MM, et al. Combined fundus autofluorescence and near infrared reflectance as prognostic biomarkers for visual acuity in foveal-sparing geographic atrophy. *Invest Ophthalmol Vis Sci*. 2017;58(6):BIO61–BIO67.
59. Sauer L, Vitale AS, Milliken CM, Modersitzki NK, Blount JD, Bernstein PS. Autofluorescence lifetimes measured with fluorescence lifetime imaging ophthalmoscopy (FLIO) are affected by age, but not by pigmentation or gender. *Transl Vis Sci Technol*. 2020;9(9):2.